Advancing High-Power Hollow-Core Fiber Pulse Compression

Maksym Ivanov, Étienne Doiron, Marco Scaglia, Pedram Abdolghader, Gabriel Tempea, François Légaré, Carlos A. Trallero-Herrero, Giulio Vampa, and Bruno E. Schmidt

(Invited Paper)

***Abstract*—Ultrafast laser science witnesses a transformative change due to the introduction of robust, high repetition rate Yb based solid state lasers. We prove the ability of hollow-core fiber (HCF) post compression to keep pace with the constantly raising average powers and pulse energies provided by state-of-the-art lasers. Over a wide range of input parameters, HCFs can provide high transmissions in the 80%–90% range with greater than 10-fold compression. First, we describe a double stage HCF setup that compresses 80 W, 2 mJ, 338 fs pulses centered at 1030 nm down to sub-two optical cycles (6 fs FWHM) with 56 W output power. This 56-fold pulse compression is paired with an overall throughput of 70% and very good long term stability (1.5% StDev over 8 hours). Next, power scaling to 300 W with variable pulse energy and repetition rate (from 100 kHz, 3 mJ to 25 kHz, 12 mJ) is presented. We compressed 1.3 ps pulses of down to 100 fs in a single HCF at 300 W level. Finally, we reveal the potential of utilizing the ultrabroadband HCF output as a spectroscopy platform that can provide various, simultaneous outputs covering a wavelength range from 430 nm up to 12 μm.**

***Index Terms*—Few-cycle, hollow-core fiber, infrared pulse generation, laser, nonlinear optics, optical frequency conversion, optical parametric amplifiers, optical pulse compression, self-phase modulation, spectral broadening, ultrashort pulse.**

Manuscript received 6 March 2024; revised 12 June 2024; accepted 12 June 2024. Date of publication 17 June 2024; date of current version 10 July 2024. This work was supported in part by The National Research Council of Canada Industrial Research Assistance Program (NRC IRAP), in part by National Research Council of Canada Challenge Program, in part by Innovative Solutions Canada, in part by the Office of Naval Research Ultra-short pulse laser and atmospheric characterization DURIP under Grant N00014-18-1-2872 and Grant N00014-19-1-2339, and in part by AFOSR under Grant FA9550-21-1-0387. *(Corresponding author: Maksym Ivanov.)*

Maksym Ivanov is with the few-cycle Inc., Varennes, QC J3X 1P7, Canada, and also with the Institut National de la Recherche Scientifique (INRS), Varennes, QC J3X 1P7, Canada (e-mail: ivanov@few-cycle.com).

Étienne Doiron, Marco Scaglia, Pedram Abdolghader, Gabriel Tempea, and Bruno E. Schmidt are with the few-cycle Inc., Varennes, QC J3X 1P7, Canada.

François Légaré is with the Institut National de la Recherche Scientifique (INRS), Varennes, QC J3X 1P7, Canada.

Carlos A. Trallero-Herrero is with the Department of Physics, University of Connecticut, Storrs, CT 06269 USA.

Giulio Vampa is with the Joint Center for Extreme Photonics, University of Ottawa, Ottawa, ON K1N 0R6, Canada, and also with the National Research Council of Canada, Ottawa, ON K1N 0R6, Canada.

Color versions of one or more figures in this article are available at https://doi.org/10.1109/JSTQE.2024.3415421.

Digital Object Identifier 10.1109/JSTQE.2024.3415421

I. Introduction

LASER technology based on ytterbium doped gain media is enjoying increasing popularity due to its multiple unprecedented advantages as compared to customary TiSa lasers. Kilowatt-level average powers [1] in a rugged and compact format, crowned by excellent stability seems to not leave much to be desired, if it weren't for the only scarcity - the limited gain bandwidth. This deficiency gave a huge push to the development of pulse post compression schemes. All popular schemes rest upon a two-step process firstly employing a nonlinear spectral broadening prior to a subsequent phase compensation. In almost all cases phase compensation is carried out with chirped mirrors (CM) [2]. Differences exist in the spectral broadening step. The longest traditions have HCFs whose energy level was boosted to the sub-mJ level for the first time in 1996 [3], [4] by using hollow fused silica capillaries. Very recent alternatives arose through the use of multi-pass cells (MPC) [5], and multiple thin plates [6]. The current record performances of the MPCs include demonstrations of sub-50 fs pulses with 200 mJ, 1 kW [7], 1 mJ, 1 kW [8] and 112 mJ with 500 W average power [9]. When it comes to few-cycle pulses, MPCs have reached 9.6 fs at 6.7 mJ however with only 6.7 W of average power [10], 5.8 fs were reached at 1 mJ with 107 W with 60% transmission in Ref. [11]. Even though the repetitive beam folding in MPCs is a very successful strategy for accumulating self-phase modulation (SPM), it leads to excessive optical path lengths thereby making optical synchronization much more challenging. With its order of magnitude shorter optical beam path, HCFs have also proven to be scalable in terms of average power and peak power. Thanks to the invention of long, stretched HCF [12], significant power scaling became possible. Recently, 70 mJ of input energy at 1030 nm [13] and 580 W average power with 5.8 mJ energy [14] have been demonstrated. In terms of transmission efficiency, HCFs still denote the best option for efficient few-cycle pulse generation, especially at elevated energies and at the 100 W level of average power. Besides spectral broadening for pulse-post compression, HCF provides a versatile platform for ultrafast, nonlinear experiments. the broad bandwidth of the spectrum after the HCF enables unprecedented overall optical efficiencies of intrapulse mid-infrared difference frequency generation [15]. Extreme pulse self-compression to sub-cycle pulses (1.2 fs) with 43 GW of peak power was demonstrated in HCF [16],

[17]. Generation of high-energy UV pulses in HCF through emission of dispersive waves [16] or through four-wave mixing of ultrashort pump and seed pulses in HCF with conversion efficiencies reaching 50% [18], [19], [20] was demonstrated. Broadband output of the HCF is used for applications in coherent spectroscopies [21]. HCF is a key technology for efficient attosecond pulse generation via the high-harmonic process in noble gases [22], [23].

The goal of this work is to report our progress using the stretched HCF technique to upscale the average power and pulse energy of HCF pulse compression systems. Firstly, double-stage pulse compression of a 100 cycle (340 fs), 80 W, 2 mJ input beam down to 1.7 optical cycles with 70% overall efficiency is presented in Sections II and III. In Section IV, we continue with the demonstration of peak and average power scaling to the 12 mJ, 300 W input level in a single stage where 1.3 ps pulses are shortened to 100 fs. A single HCF setup supports variable input repetition rate between 100 kHz (3 mJ) and 25 kHz (12 mJ) at 300 W level. We conclude with an outlook in Section V showing how the ultra-broadband HCF output can be utilized to drive different frequency mixing stages that yield simultaneous, optically synchronized outputs in the UV and up to the far IR range at 12 μm. In general, we prove that effects due to the beam pointing drifts can be eliminated with an economical stabilization system, hence enabling constant operation over many months at a few-hundred watts of average power level.

II. Pulse Compression of a 2 mJ, 80 W, 338 fs Yb-Laser Down to 28 fs With 86% Transmission

The starting point is Yb:KGW regenerative amplifier (Carbide, Light Conversion) delivering 80 W, 2 mJ pulses at 40 kHz repetition rate with a pulse duration of 338 fs. The laser beam is focused with a lens to 65% of the fiber diameter to reach optimum coupling into the fundamental mode of 700 μm inner diameter (ID) HCF (few-cycle Inc). The choice of the 700 μm inner diameter for the HCF was made based on an empirically determined compromise between highest transmission (achieved with larger cores) and optimum mode quality. While large cores of 750um or even 1000 μm enable higher transmission, we observed slight mode degradation when pushing for all three aspects combined: i) a high nonlinearity required for compression ratios greater than 8-10 paired with ii) high peak and iii) high average power. If one of the three aspects is not required, larger cores than 700 μm become relevant again. A fourth optimization parameter iv) is the fiber length. While a longer propagation length allows operation at lower gas pressure to achieve the same compression factor it might lead to space conflicts. A fiber that is too short, on the other hand, causes a fast accumulation of the nonlinear phase, leading to higher-order chirps and, thus, higher pedestals in the compressed pulse. To achieve cleaner compressed pulses, one has to balance SPM with GVD [24], [25]. This, in turn, is increasingly difficult with larger cores where the GVD becomes almost negligible. To find a good balance between the different and partially opposing requirements, we experimentally tested 80, 160, and 210 cm long HCFs with different IDs of 500 μm and 700 μm. Under the given input laser parameters and desired

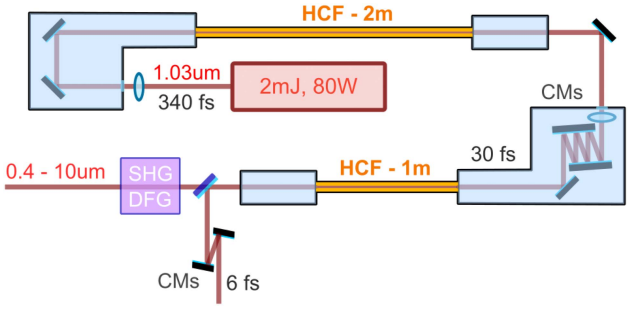

Fig. 1. Sketch of the experimental setup. The light blue sections denote vacuum chambers filled with noble gas to reduce propagation effects in air. The inner diameter of both hollow-core fibers (HCFs) is 700 μm and their respective lengths are 2 m and 1 m. CMs – chirped mirrors; SHG, DFG – second harmonic generation and difference frequency generation addons.

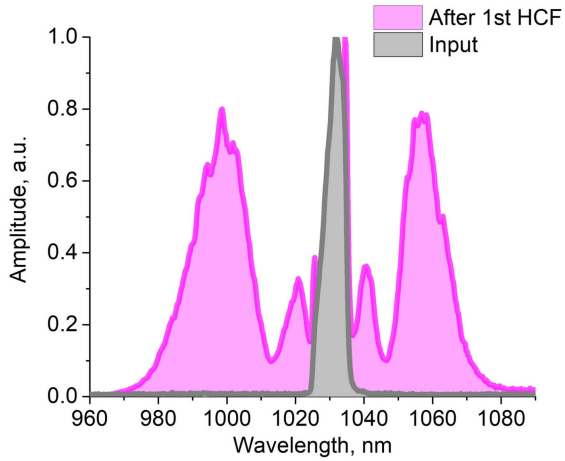

Fig. 2. Spectral characterization. The input spectrum (gray) versus the broadened spectrum (magenta) out of a 2.1 m long, 700 μm ID fiber with close to 90% transmission. HCF is filled with 2.4 bar of absolute pressure of argon.

compression factor, a 2-meter long HCF with a 700 μm ID was the best choice to achieve fairly clean compressed pulses with minimal pedestals and maximum throughput. The choice of the gas type and pressure was made based on the nonlinearity required to achieve desired spectral broadening and input beam parameters. For the given input laser parameters and fiber diameter, 2.4 bar of Argon or 1 bar of Krypton is suitable.

To avoid beam propagation issues in air, the beam travels inside a vacuum beam delivery system right after the focusing lens, as shown in Fig. 1. Because of the high average power, which causes heating of the optical mounts and components, and temperature variations in the lab, the beam is susceptible to thermal drifts over the day. To compensate for the slow drift of the beam position, we have developed a compact beam stabilization system consisting of a CMOS camera and motorized mirror mount. The feedback loop of the beam drift compensation system operates at 1 Hz repetition rate, which is fully sufficient to compensate thermal drifts.

The HCF is filled with argon at 2.4 bar absolute pressure (1.4 bar relative) and the broadened spectrum after 2.1 m of propagation in the HCF is shown in Fig. 2 as the magenta curve and is overlapped with the input spectrum (gray). The more than 10-fold broadened spectrum exhibits the typical, fairly

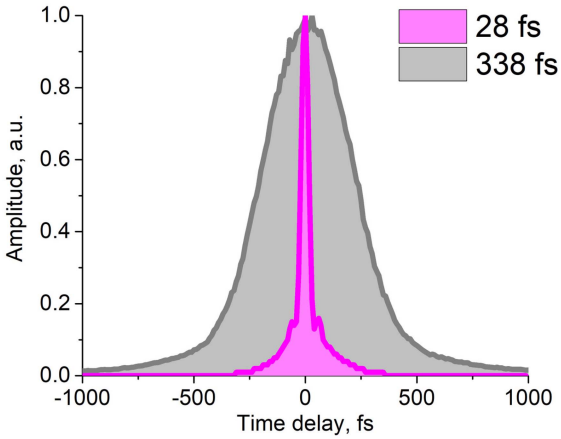

Fig. 3. Temporal characterization. Autocorrelations show the 12-fold pulse compression after the first HCF stage (magenta) versus the input pulse duration (gray).

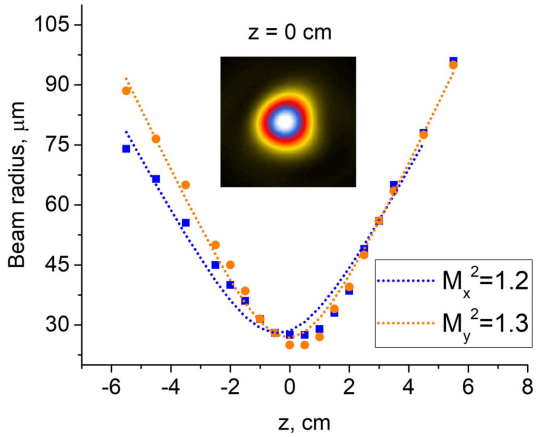

Fig. 5. Beam shape and M^2 measurements after the first HCF. Inset shows the beam shape at the focus.

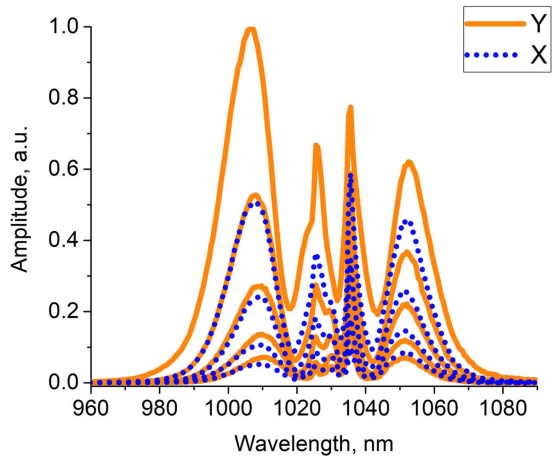

Fig. 4. Spatial homogeneity (spatial chirp) of spectral broadening in the first HCF. Data points are taken at X, mm and Y, mm corresponding to 100%, 50%, 25%, 12% and 6% of the beam intensity.

symmetric features of SPM. The sharp remaining central peak is attributed to uncompensated higher order phases of the laser source and may be connected to the small deviation from a purely Gaussian temporal pulse envelope as it is shown as the gray curve in Fig. 3. With a fiber transmission close to 90%, the total transmitted power after the chirp mirrors and transport optics is 68 W, which corresponds to 1.7 mJ of pulse energy at 40 kHz repetition rate, denoting a total transmission of the pulse compression setup of 86%.

To investigate the presence of spatial chirp, we quantified the spatial homogeneity of the spectrum by scanning a small fiber coupled to a spectrometer (Avantes AvaSpec-Mini4096CL-UVI10) across the beam profile. The results in Fig. 4 show the spectral shape along the vertical (dotted blue) and horizontal (orange) directions of the beam profile at different points as indicated by the legend. The absence of spatial chirp is accompanied by a good focus, shown in the inset in Fig. 5. The corresponding M^2 measurements reveal values of 1.2 and 1.3, respectively, which are slightly higher than the ones of the laser (1.15) at full power. The temporal characterization is carried out by performing autocorrelation measurements which are shown in Fig. 3. The plot of the input pulse duration of 338 fs at Full Width at Half Maximum (FWHM) (gray curve) is overlaid with the one of the compressed 28 fs at FWHM pulse (magenta curve). The phase compensation required for this 12-fold compression is performed with 10 bounces off the chirped mirrors (-200 fs^2 at 960–1100 nm, few-cycle Inc). From the magenta curve in Fig. 3, one can see that the main pulse is flanked by pedestals. Their origin has yet to be identified. To investigate this, as a first test, we reduced the repetition rate from 40 kHz to 4 kHz by a pulse picker, i.e., the average power was reduced by a factor of 10 without changing any other parameter. Since we did not observe any change, this confirms that the pedestals are not related to the average power. In turn, this means that even though the HCF setup is only passively cooled, 80 W of the incident power has no effect on the temporal pulse quality. On the other hand, reducing the gas pressure and increasing the pulse duration does lead to cleaner pulse shapes with less pedestals.

Besides the 10-fold increase in pulse power, stability of the system, both, on a shot-to-shot basis and on the long term is a key factor for many applications. The shot-to-shot stability was measured over an extended time span of 30 minutes. Every shot was analyzed at 40 kHz repetition rate of the laser. The result, which is shown in Fig. 6, reveals an extremely low standard deviation of 0.27% over about 7.2×10^7 individual pulses. The HCF compression system marginally increased the standard deviation by adding only 0.17% of shot-to-shot noise to the laser fluctuations. This could be caused by such effects around the laser focus in the vicinity of the fiber entrance as micro-ablation, heat convection, and mechanical vibrations. The presented HCF stabilities compare well to that of state-of-the-art MPC compression systems at comparable power levels, which can be as low as 0.247% standard deviation of energy fluctuations [11]. We believe that one key element for reaching this record shot-to-shot stability is the implementation of a tapered ceramic protection which is directly attached to the hollow fused silica waveguide. We hypothesize that the grazing incident angle, as compared to a perpendicular hit in case of a straight ceramic protection cap, helps to reduce unavoidable micro ablations in the vicinity of

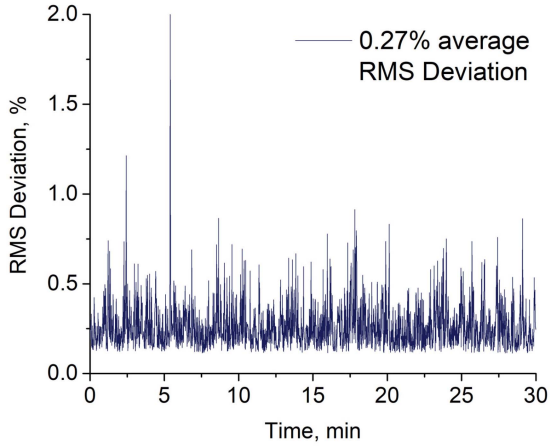

Fig. 6. Shot-to-shot power stability taken with a photodiode after the first HCF reveals 0.27 % RMS Deviation averaged over 30 min.

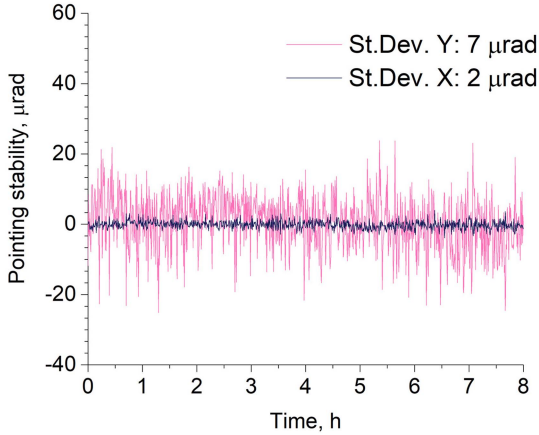

Fig. 7. 8 h long pointing stability after the first HCF.

the laser focus. These micro ablations are probably causing an increasingly stronger impact as the peak power or average power, respectively, rises. Further detailed investigations on these subtle aspects of the fiber coupling under extreme conditions are on the way. Certainly, another key prerequisite for this excellent stability was the remarkable performance of the input laser. The Yb laser's shot-to-shot stability, evaluated in the same manner, yielded a standard deviation of less than 0.1%.

Due to this highly stable performance, the compressed pulses are ready to be applied to other challenging nonlinear optical experiments. In our case, the application was to drive a subsequent HCF with the goal to achieve mJ-level few-cycle pulses. In view of applications, it is worth stressing that at this combination of peak -and average -power (60 GW and 60 W) pulse propagation in air is likely to cause spatial beam distortions. One way to circumvent this is to increase the beam size to reduce the intensity. The amount of spatial beam distortion depends on many factors: the average power, the pulse energy, the pulse duration and the propagation length in air.

III. Sub-2 Cycle (6.1 fs) Pulse Compression of a 2 mJ, 80 W, 338 fs Yb-Laser With 72% Transmission

Because we wanted to minimize the overall optical beam path of the two-stage HCF setup, we decided to keep the beam diameter small, about 5 mm at $1/e^2$ of intensity at the largest point. This requires performing pulse compression under vacuum or low-pressure inert gas atmosphere. The beam path between chirp mirrors and the second HCF was kept under a low pressure argon atmosphere. The pressure was defined by the nonlinear operation conditions for the 2nd HCF and ranged between 0.4 - 0.7 bar of absolute pressure. Different combinations of fiber lengths (0.8 m, 1 m, and 1.6 m) and fiber diameters were tested to find the most compact compromise between high throughput, maximum operational energy (1.7 mJ), and sufficient spectral broadening to support 2-cycle pulses while keeping the HCF length minimal.

We settled on a design employing a 1 m long, 700 μm ID HCF. It enabled a fiber throughput of 85% at maximum peak and average power. With this combination, the total setup length including input coupling and output collimation was 3.6 m which is the same as for the first HCF. In comparison, the 1st HCF, which does the heavy lifting of >10-fold compression, has the same ID but is twice as long. But since the peak power is lower in the first stage, the in – and out coupling arms can be more compact. Employing a smaller ID HCF in the 2nd stage would lead to a more compact design but so far only enabled us to reach 80% transmission at full power. To reach our target of 70% overall transmission of the double stage compressor, we chose the larger core option of 700 μm.

Like in the case of the 1st HCF, the beam pointing into the 2nd fiber was actively stabilized with a slow drift compensation. Fig. 7 shows the pointing stability of the beam coupled into the 2nd HCF. While the tiny fluctuations of 2 urad along the horizontal are insignificant, larger fluctuations are visible in the perpendicular direction. The origin of this effect is not yet fully confirmed but we believe it is due to the readout noise of our CMOS camera. Although we do not think it contributes significantly to the fiber stability, since the data for the first pointing system is similar, we aim to eliminate this presumably electronically-caused noise in future.

The output beam was characterized in a manner similar to the case of the first HCF. Rather symmetric broadening reaching from 700 nm up to 1250 nm was observed. All spectra are overlaid for comparison in Fig. 8 (cyan color for 2nd HCF output). To detect full bandwidth of the broadened spectrum two spectrometers were used. One is sensitive in the range 200–1100 nm (Avantes AvaSpec-Mini4096CL-UVI10) and another one is sensitive in the range 900–1700 nm (Avantes AvaSpec-NIR256-1.7-HSC-EVO). Spectra from both spectrometers were matched in the region of overlap and stitched together to demonstrate continuous output of the second HCF. Even though an M^2 measurement was not yet available, a first test of the spatial chirp indicated a nicely uniform distribution of the ultra-broadband output, as is seen in Fig. 9. The horizontal and vertical scans show no sign of the spatial chirp. Due to the limited spectral range of the silicon detector (Avantes AvaSpec-Mini4096CL-UVI10), only the blue spectral part is well represented in this measurement. The curves correspond to the center of the beam, 50, 25,

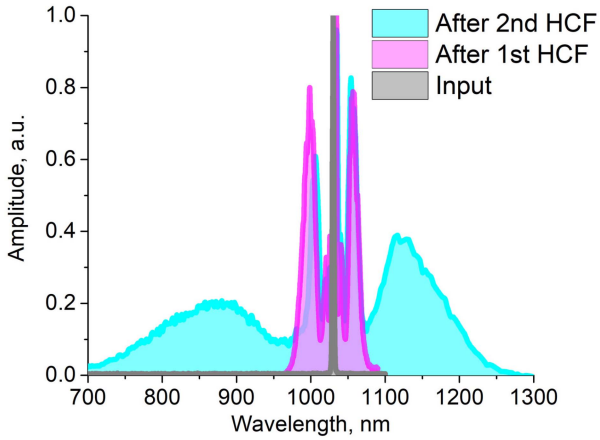

Fig. 8. Spectral characterization. Spectral broadening in the second HCF (cyan) versus input spectrum after the first HCF stage (magenta), with the spectrum out of the laser (gray).

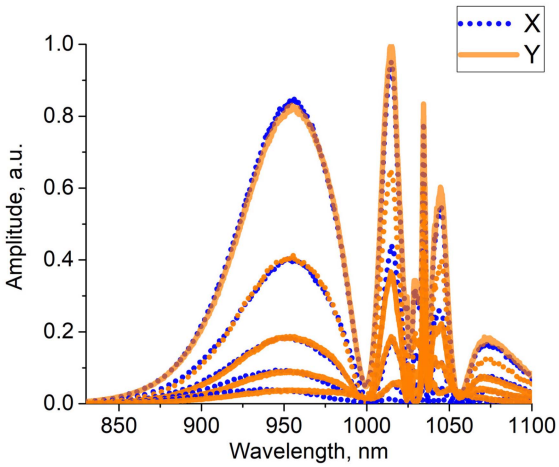

Fig. 9. Spatial homogeneity (spatial chirp) of spectrum after the second HCF. Data point are taken at X, mm and Y, mm corresponding to 100%, 50%, 25%, 12% and 6% of the beam intensity.

12 and 6% of the maximum intensity level and demonstrate excellent spatial quality of the spectral broadening. Spectra shown through out the manuscript have rough corrections for the spectrometer sensitivity, which might be more inaccurate closer to the end of the sensitivity range of the spectrometer. That is why spectral peaks in Fig. 9 have very different amplitudes. On the contrary, Fig. 8 shows well-corrected spectra obtained from two spectrometers having different spectral ranges, which are stitched together.

After compression with chirped mirrors (-58 fs^2 at 600–1250 nm, few-cycle Inc) FWHM pulse duration of 6.1 fs is obtained (Fig. 10, cyan colored). To avoid beam propagation issues, the temporal characterization was carried out with a wedge reflection, instead of the full beam. Considering the losses on the chirped mirrors, windows, fiber, and guiding optics we achieved 56 W, 1.4 mJ pulses at 40 kHz. It was demonstrated that an equal (minimal) compression factor per stage could improve a temporal contrast of the generated pulses by minimizing the higher-order chirp [26]. Such optimization of the double stage pulse contrast enhancement will be carried out in future. For

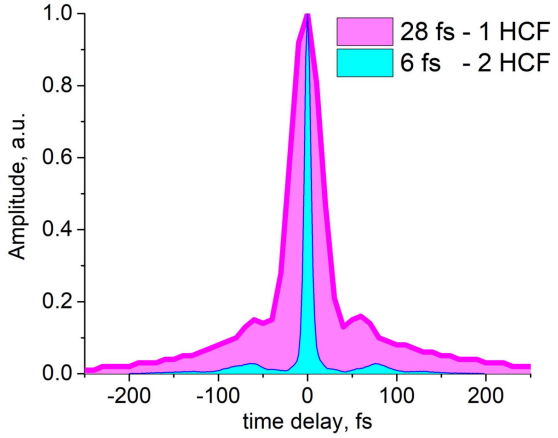

Fig. 10. Spectral characterization. Autocorrelation showing pulse duration after the second HCF, 6 fs (cyan), versus the input pulse duration after the first HCF, 28 fs (magenta).

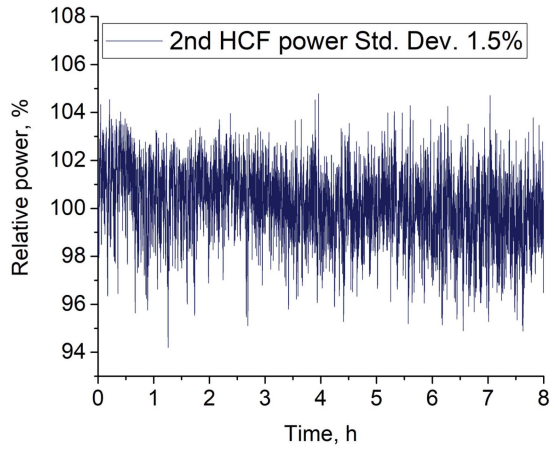

Fig. 11. Power stability of second HCF over 8 h with Standard Deviation of 1.5 %.

this experiment, however, our goal was to demonstrate >10-fold single stage compression yielding sub-30 fs pulses, which is not readily available from other compression techniques, such as MPCs, at comparable input energies.

Preliminary data for the long term power stability for the entire double stage HCF setup is presented in Fig. 11. The power recorded over 8 hours with a power meter exhibits a standard deviation of 1.5%. A slight drop of 1% is noticeable. One reasonable explanation is, that for both HCFs, the corresponding fiber entrances and exits are placed on different optical tables that are only weakly connected. Regardless of these small technical shortcomings, the double stage HCF system is stable enough to serve as the starting point to drive secondary sources. In Section V, we give an outlook and apply the ultra-broad band output for subsequent frequency mixing.

IV. Pulse Compression of 300 W, 12 mJ With 83% Transmission in Air Cooled Hollow-Core Fiber

In this section we take advantage of the versatility our stretched HCF setup offers by means of two examples: power scaling and repetition rate switching. Regarding the first, we

demonstrate that by utilizing largely the same hardware as in the 80 W experiment, it is possible to raise both the input average power to 300 W as well as the pulse energy to 12 mJ. While high energy is required to drive extreme light matter interactions on the one hand, it is unavailing in many other cases like for instance angular resolved photo electron spectroscopy [27]. Thus, to drive very different types of ultrafast experiments, high power lasers and the successive compression stages should support repetition rate switchable outputs. In the ideal scenario, higher repetition rate can be traded against lower energy and vice versa by keeping the average power constantly high. To facilitate the power scaling, an Yb:YAG InnoSlab (Amphos) was used. This laser can deliver a variable combination of pulse energy and repetition rate while keeping the average power constant at 300 W. The maximum energy at 25 kHz is 12 mJ with a pulse duration of 1.26 ps. With this input we achieved simultaneous upscaling of average power and pulse energy to 250 W and 10 mJ at the HCF output. This denotes to date the highest energy pulse compression in HCFs at the multi-hundred-Watt level.

The beam was coupled in a loose focusing condition (2.8 m focal length lens). Behind the lens, all beam routing was carried out under the same noble gas pressure that the HCF was operated with. The HCF is 3.1 m long, which is the minimum length necessary to achieve desired broadening and clean compressed pulses. To have less heat deposited to the fiber tip we chose a high throughput - large mode fiber of 1 mm inner diameter. This type of HCF has proven to enable up to 97% transmission with a low power Yb regenerative amplifier delivering 1 mJ input with 6 W average power [28]. Because we used a longer fiber and due to the challenging average power and focal spot behavior of the InnoSlab laser (discussed in more details in the end of this section) we achieved a reduced HCF transmission of about 83% with 300 W input. Before achieving this result, we had to carefully characterize the small but noticeable changes of the focal spot when ramping up the average power and when switching the repetition rate. Aside from the large core, the main difference compared to the 80 W setup is that the entrance fiber tip (not the entire fiber) was actively cooled with a low flow of ambient air only. Water cooling is not required at this average power level.

In the first experiment, we operate the HCF at 100 kHz, 3 mJ of input energy keeping the power at 300 W. The broadened spectrum after propagation in 2.5 bar of krypton absolute pressure (1.5 bar relative) the broadened spectrum is shown in Fig. 12 as magenta curve overlapped with the input spectrum (gray). SPM-like spectral broadening has a central peak which we attribute to the input pulse pedestals of the Yb laser, which doesn't contribute to SPM. The pedestals reach out to 7 ps which is not seen in Fig. 13 (gray curve) due to the selected region. Pulse compression was performed using 40 bounces on chirped mirrors (-500 fs^2 at 1010–1060 nm, few-cycle Inc). The temporal characterization by autocorrelation shows that the pulse was compressed down to 99 fs at FWHM (Fig. 13 magenta curve), which corresponds to 12-fold pulse compression at 300 W of input average power. To prove the versatility, we elevated input energy to 12 mJ (25 kHz, 300 W) as the next step. To achieve similar spectral broadening as in 100 kHz, 3 mJ case

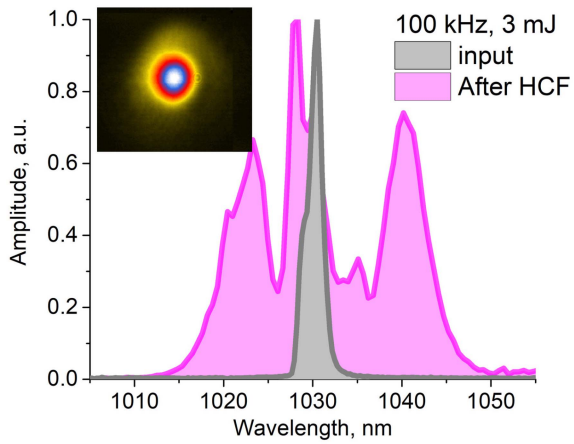

Fig. 12. Spectrum after broadening in the 3.1 m long 1 mm diameter HCF (magenta) versus input spectrum (gray) at 100 kHz. Inset demonstrates the beam refocused to the focal spot with diameter of 550 μm by 550 μm.

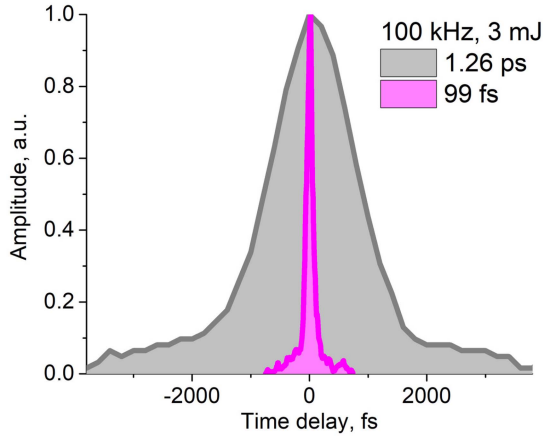

Fig. 13. Autocorrelation showing compressed pulse duration after the HCF, 99 fs (magenta), versus input pulse duration of 1.26 ps (gray) at 100 kHz.

the gas pressure in the HCF was reduced to 1.17 bar of krypton absolute pressure (0.17 bar relative pressure). Since, the focusing conditions (size, ellipticity, z-position) of the input beam slightly differ between 12 mJ and 3 mJ laser operation we had to choose an optimum compromise that still supports good fiber coupling at both situations reasonably well. The broadened spectrum after propagation in the HCF is shown as magenta curve in Fig. 14. While similar SPM-like broadening is observed, one can also recognize a higher remaining central peak, as compared to the 3 mJ case, seen in Fig. 14. We attribute this to an increase of pulse pedestals when the laser is operated at lower repetition rate with 12 mJ. Nonetheless, the pulse compression ratio is similar to the lower input energy case. To reach the shortest pulse duration a reduced number of bounces (36 instead of 40) off the same chirped mirrors (-500 fs^2 at 1010–1060 nm, few-cycle Inc) was necessary. Autocorrelation shows pulse duration of 103 fs at FWHM (magenta curve in Fig. 15). We note that only a 3.5% fraction of the power was sent over the chirp mirrors in the high energy case. For the later experiment, the large aperture (25 mm $\times$ 85 mm) chirp mirrors will be placed inside a vacuum chamber.

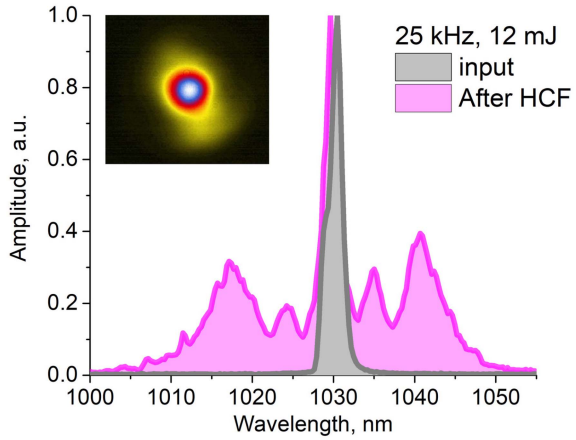

Fig. 14. Spectrum after broadening in the same 3.1 m long 1 mm diameter HCF versus the input spectrum at the repetition rate of 25 kHz and input energy of 12 mJ. Inset demonstrates the beam refocused to the focal spot with diameter of 700 μm by 800 μm.

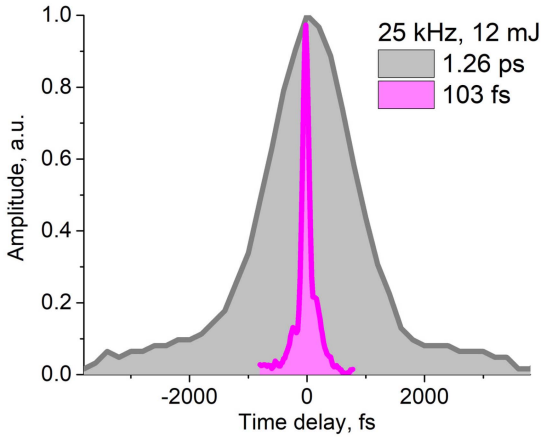

Fig. 15. Autocorrelation showing compressed pulse duration after the HCF, 103 fs (magenta), versus input pulse duration of 1.26 ps (gray) at 25 kHz.

The broadened spectra presented in Fig. 12 for 3 mJ input and in Fig. 14 for 12 mJ input show different bandwidth necessary to compress the pulses down to 100 fs. This might be caused by a larger B-integral and/or higher-order chirp already accumulated in the laser before the HCF in the 12 mJ case. Furthermore, broadening with the 12 mJ input is closer to the gas ionization in the HCF than in the 3 mJ case, which might cause the beginning of blue shifting of the spectrum. These effects might explain the slightly higher pedestals visible in the autocorrelation in Fig. 15 (12 mJ) compared to Fig. 13 (3 mJ) and the slight asymmetry of the focus after the HCF in the high-energy case.

The spatial quality of the beam after the HCF was verified by refocusing the beam after the HCF. The beam was refocused with a lens of 1 m focal length to a focal spot with the diameter of 750 μm by 750 μm in the case of the 3 mJ input (inset in Fig. 12) and to 700 μm by 800 μm focal spot in the case of 12 mJ (inset in Fig. 14). Visible halo around the focused beam could be originating from two sources. i) contribution from the miscoupling of the astigmatic focus of the input laser

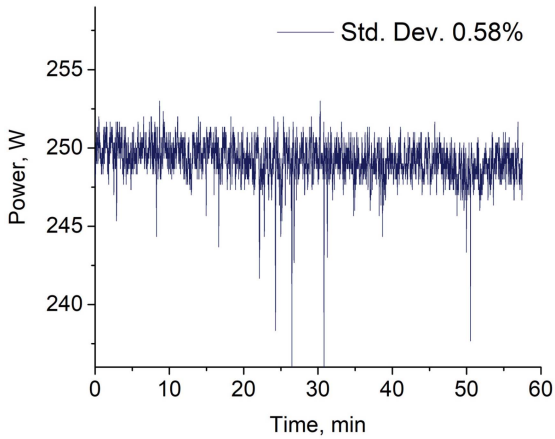

Fig. 16. One hour power stability of the HCF output revealing Standard Deviation of 0.58%. Data is taken with 300 W, 12 mJ, 25 kHz input to the HCF.

beam to the HCF: beam coming directly from the laser has its X and Y axes focus at different distances after the lens with X axis being $\sim 25\%$ smaller than the Y axis. ii) contribution from the higher order modes of the large core hollow-core fiber.

Fig. 16 shows a stable 1-hour long power measurement with a remarkably low standard deviation of 0.58% at 250 W of average power at 25 kHz.

V. VIS to IR Frequency Shifting

In this section we briefly outline how ultra-broadband spectra of the sub-two cycle pulses described in Section III can be further exploited. Pump-probe type of experiments denote the very foundation of ultrafast science. Besides changing the pulses arrival time on the sample, spectroscopists also appreciate the ability to change the pulse frequencies. To realize this with a typical 50 fs time resolution, optical parametric chirped-pulse amplifiers (OPCPAs) or non-collinear optical parametric amplifiers (NOPAs) have been used. If pump and probe pulses require different frequencies, one has to implement and synchronize different OPAs. However, this challenge could be approached differently. In this case, the ultrabroadband output serves as the steppingstone for subsequent difference frequency (DFG) and second harmonic generation (SHG) stages. The SPM spectral sidebands naturally exhibit a linear phase. Thus, spectrally selecting sidebands of the spectrum shown in Fig. 8 in the ranges 700–960 nm and 1080–1250 nm yields close to transform-limited sub-40 fs pulses. Therefore, their frequency mixing directly produces short pulses across the spectral tuning range. Subsequent chirp compensation is not required like in the case of OPCPAs or NOPAs.

To access visible, UV and IR wavelengths with two separately tunable channels, the ultra-broadband HCF spectrum (Fig. 17 cyan colored) is separated by means of a dichroic beam splitter into wavelengths shorter and longer than 1030 nm. The separation is done before the chirped mirrors as the pulse compression for this purpose is not necessary. Two beams after the dichroic with the spectral ranges between 700–960 nm and

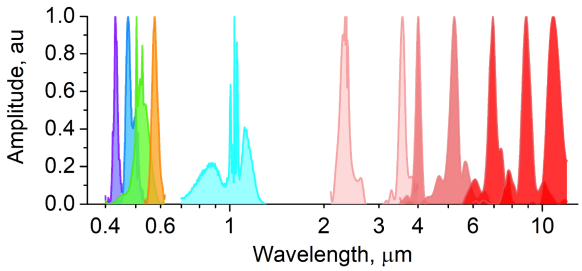

Fig. 17. Frequency tuning of the HCF output by generating SH (rainbow colored) and DFG (shaded red) between spectral components of the fundamental spectrum around 1 μm wavelength (cyan). Log scale is used for the horizontal.

1080–1250 nm were sent onto two BBO crystals for SHG. The two independently frequency tunable outputs provide sub-50 fs pulses in the visible range from 400 nm to 600 nm (Fig. 17, violet, blue, green, and orange colored). A full characterization of the UV-VIS light source characteristics is currently underway. The total conversion efficiency calculated as the laser output into a single VIS beam is about 3–5 % at the peak wavelengths of 450 nm and 560 nm, yielding 2.5 W and 4 W of average power, respectively. The results demonstrate first attempts on creating ultra-broadband frequency tunable platform and efficiency of conversion would be improved. To extend the range further into UV, another SHG step could be implemented that will upconvert the 50 fs visible pulses to a range from 225–280 nm. Wavelengths between 300 nm and 430 nm could be accessed through sum frequency mixing of the broadband HCF output and its SH. Numerical calculations show that it should be possible to frequency double most of the full sub-3 cycle pulse spectrum at 1030 nm at once to achieve sub-10 fs at 515 nm in a 30–50 μm thick BBO crystal.

To fully exploit the opportunities given by the ultra-broadband HCF output spectrum with its flat spectral phases across the two spectral sidebands, we performed DFG between the sidebands. About 2% of the HCF output was split off for this purpose. The same dichroic beam splitter as above was used to separate 700–960 nm and 1080–1250 nm spectral ranges into two separate beams. After dichroic beam splitting and colinear recombination, about 800 mW of power was incident on the IR-DFG crystals. Fig. 17, depicted in red, shows the normalized spectra of the DFG output between 2 and 12 μm. Different crystals were tested for the generation of DFG. The best conversion efficiencies were achieved with an AGS crystal in the range of 6–12 μm, LiIO3 in the range of 4–5 μm, and LiNbO3 for the 2–4 μm range (shown by shaded red colors in Fig. 17). Noteworthy, despite the ultrabroadband spectrum, about 0.15-0.2% of DFG conversion efficiency was measured into the mid-IR range from 6-12 μm from the 800 mW pump beam with at least two times better efficiencies in the 2–5 μm range. Since 12 μm is the current limit of our IR spectrometer (ARCoptix FT-IR Rocket), we are not able to tell if the spectrum could be extended further. Since, only 2% of the HCF output was used for the generation of the IR pulses, their power could be boosted by using a larger fraction of the beam.

Following this approach one could obtain universal platform with simultaneous outputs at UV, VIS, NIR and far IR ranges with sub-100 fs pulse durations whose time synchronization is facilitated by short optical distances to the laser source.

VI. Conclusion

We report on the average power and energy scaling with hollow-core fibers. First, we demonstrate 12-fold compression of 80 W, 2 mJ, 338 fs pulses down to 28 fs with 86% efficiency. A remarkable shot-to-shot stability of 0.27% was measured over 7×10^7 individual laser shots (30 min at 40 kHz). This output was sent to a subsequent HCF. Both cascaded HCFs together yielded 55-fold compression down to 6.1 fs with 70% of the total transmission, which corresponds to 1.4 mJ pulse energy at 56 W of average power. No active fiber cooling is necessary at the 100 W level. Further, power upscaling to 300 W, 12 mJ was demonstrated with more than 80% transmission. Employing a single fiber setup a high degree of user flexibility was realized. The setup, allowed to vary the repetition rate between 100 kHz (3 mJ) and 25 kHz (12 mJ) at 300 W level with constant 10-fold pulse compression from 1.26 ps to 100 fs. Thanks to the high transmission through the HCF, thermal effects at 300 W level are kept at a minimum. Additionally, the design of the fiber tip allows for auxiliary active heat dissipation with a minimum flow of ambient air. Further average power scaling to 1 kW would denote potential loss of 150 W for the fiber with 85% transmission. To simulate this situation we detuned the fiber coupling to increase transmission losses and successfully tested the evacuation of 150 W with an upgraded fiber cooling setup. The thermal stress tests indicate feasibility of average power scaling to the 1 kW level.

In addition to pulse compression, we introduce the double stage HCF broadening of a narrowband Yb laser as a versatile platform for the simultaneous generation of tunable visible to mid-infrared wavelengths, with the work in progress to extend it to ultraviolet.

References

[1] Y. Wang et al., "1.1 J Yb:YAG picosecond laser at 1 kHz repetition rate," *Opt. Lett.*, vol. 45, no. 24, pp. 6615–6618, 2020.
[2] R. Szipöcs, K. Ferencz, C. Spielmann, and F. Krausz, "Chirped multilayer coatings for broadband dispersion control in femtosecond lasers," *Opt. Lett.*, vol. 19, no. 3, pp. 201–203, 1994.
[3] M. Nisoli, S. De Silvestri, and O. Svelto, "Generation of high energy 10 fs pulses by a new pulse compression technique," *Appl. Phys. Lett.*, vol. 68, no. 20, pp. 2793–2795, 1996.
[4] S. De Silvestri, M. Nisoli, G. Sansone, S. Stagira, and O. Svelto, "Few-cycle pulses by external compression," *Topics Appl. Phys.*, vol. 95, pp. 137–178, 2004.
[5] J. Schulte, T. Sartorius, J. Weitenberg, A. Vernaleken, and P. Russbueldt, "Nonlinear pulse compression in a multi-pass cell," *Opt. Lett.*, vol. 41, no. 19, pp. 4511–4514, 2016.
[6] C.-H. Lu et al., "Generation of intense supercontinuum in condensed media," *Optica*, vol. 1, no. 6, pp. 400–406, 2014.
[7] Y. Pfaff et al., "Nonlinear pulse compression of a 200 mJ and 1 kW ultrafast thin-disk amplifier," *Opt. Exp.*, vol. 31, no. 14, pp. 22740–22756, 2023.
[8] C. Grebing, M. Müller, J. Buldt, H. Stark, and J. Limpert, "Kilowatt-average-power compression of millijoule pulses in a gas-filled multi-pass cell," *Opt. Lett.*, vol. 45, no. 22, pp. 6250–6253, 2020.
[9] M. Kaumanns, D. Kormin, T. Nubbemeyer, V. Pervak, and S. Karsch, "Spectral broadening of 112 mJ, 1.3 ps pulses at 5 kHz in a LG_{10} multipass cell with compressibility to 37 fs," *Opt. Lett.*, vol. 46, no. 5, pp. 929–932, 2021.

[10] S. Rajhans et al., "Post-compression of multi-millijoule picosecond pulses to few-cycles approaching the terawatt regime," *Opt. Lett.*, vol. 48, no. 18, pp. 4753–4756, 2023.
[11] S. Hädrich et al., "Carrier-envelope phase stable few-cycle laser system delivering more than 100 W, 1 mJ, sub-2-cycle pulses," *Opt. Lett.*, vol. 47, no. 6, pp. 1537–1540, 2022.
[12] T. Nagy, M. Forster, and P. Simon, "Flexible hollow fiber for pulse compressors," *Appl. Opt.*, vol. 47, no. 18, pp. 3264–3268, 2008.
[13] G. Fan et al., "70 mJ nonlinear compression and scaling route for an Yb amplifier using large-core hollow fibers," *Opt. Lett.*, vol. 46, no. 4, pp. 896–899, 2021.
[14] T. Nagy et al., "Generation of three-cycle multi-millijoule laser pulses at 318 W average power," *Optica*, vol. 6, no. 11, pp. 1423–1424, 2019.
[15] Q. Bournet et al., "Inline amplification of mid-infrared intrapulse difference frequency generation," *Opt. Lett.*, vol. 47, no. 19, pp. 4885–4888, 2022.
[16] J. C. Travers, T. F. Grigorova, C. Brahms, and F. Belli, "High-energy pulse self-compression and ultraviolet generation through soliton dynamics in hollow capillary fibres," *Nature Photon.*, vol. 13, pp. 547–554, 2019.
[17] C. Brahms, T. Grigorova, F. Belli, and J. C. Travers, "High-energy ultraviolet dispersive-wave emission in compact hollow capillary systems," *Opt. Lett.*, vol. 44, no. 12, pp. 2990–2993, 2019.
[18] C. G. Durfee, S. Backus, H. C. Kapteyn, and M. M. Murnane, "Intense 8-fs pulse generation in the deep ultraviolet," *Opt. Lett.*, vol. 24, no. 10, pp. 697–699, 1999.
[19] A. Lekosiotis et al., "Progress in ultrafast optics using hollow-core fibres," in *Proc. Specialty Opt. Fibers*, 2022, Paper SoTu4I.2.
[20] I. Babushkin et al., "Four wave mixing in multimode hollow core waveguides with a two-color pump for the thorium nuclear clock," in *Proc. EPJ Web Conf.*, 2022, Paper 02039.
[21] S. Palato et al., "An analysis of hollow-core fiber for applications in coherent femtosecond spectroscopies," *J. Appl. Phys.*, vol. 128, no. 10, 2020, Art. no. 103107.
[22] A. Baltuška et al., "Attosecond control of electronic processes by intense light fields," *Nature*, vol. 421, pp. 611–615, 2003.
[23] I. Thomann et al., "Characterizing isolated attosecond pulses from hollow-core waveguides using multi-cycle driving pulses," *Opt. Exp.*, vol. 17, no. 6, pp. 4611–4633, 2009.
[24] H. Nakatsuka, D. Grischkowsky, and A. C. Balant, "Nonlinear picosecond-pulse propagation through optical fibers with positive group velocity dispersion," *Phys. Rev. Lett.*, vol. 47, pp. 910–913, Sep. 1981.
[25] W. J. Tomlinson, R. H. Stolen, and C. V. Shank, "Compression of optical pulses chirped by self-phase modulation in fibers," *J. Opt. Soc. Amer. B*, vol. 1, no. 2, pp. 139–149, Apr. 1984. [Online]. Available: https://opg.optica.org/josab/abstract.cfm?URI=josab-1-2-139
[26] E. Escoto et al., "Temporal quality of post-compressed pulses at large compression factors," *J. Opt. Soc. Amer. B*, vol. 39, no. 7, pp. 1694–1702, Jul. 2022.
[27] Y. Wang and M. Dendzik, "Recent progress in angle-resolved photoemission spectroscopy," *Meas. Sci. Technol.*, vol. 35, no. 4, 2024, Art. no. 042002.
[28] Y.-G. Jeong et al., "Guiding of laser pulses at the theoretical limit–97% throughput hollow-core fibers – With subsequent compression to 1.3 cycles," in *Proc. Int. Conf. Ultrafast Phenomena*, 2022, Paper Tu2B.4.

Maksym Ivanov received the bachelor's degree (with Hons.) in optics and the master's degrees (with Hons.) in quantum electronics from the Taurida National V.I. Vernadsky University, Simferopol, Ukraine, in 2011 and 2012, respectively, and the Ph.D degree in laser physics from Vilnius University,Vilnius, Lithuania, in 2019. Since 2019, he has been an Industrial Postdoctoral Researcher jointly with INRS - Institut national de la recherche scientifique, Varennes, QC, Canada, and with few-cycle Inc., Varennes, working in the field of ultrafast and nonlinear optics. His research interests mainly include pulse post compression of high-energy and high-power ultrafast lasers and nonlinear optics techniques such as optical parametric amplification.

Étienne Doiron received the B.Eng. degree in engineering physics and the M.A.Sc. degree in engineering physics from Polytechnique Montréal, Montreal, in 2018 and 2021, respectively. Since 2022, he has been a Research Scientist with few-cycle Inc., Varennes, working on ultrafast and nonlinear optics for the development of pulsed laser solutions. His research interests mainly include pulse compression of high-energy and high-power ultrafast lasers and nonlinear optics techniques such as optical parametric amplification.

Marco Scaglia received the B.S. and M.S. degrees in physics engineering from Politecnico di Milano, Milan, Italy, in 2019 and 2022, respectively, and the M.A.Sc. degree in physics engineering from Polytechnique Montréal, Montreal, QC, Canada, in 2022. Since 2023, he has been a Research Scientist with few-cycle Inc., Varennes, working in the field of ultrafast lasers and nonlinear optics. His research interests mainly include pulse compression of high-energy and high-power ultrafast lasers, and nonlinear optics applications.

Pedram Abdolghader received the bachelor's (with Hons.) and master's (with Hons.) degrees in atomic, molecular, and optical physics from the University of Tehran, Tehran, Iran, and the Ph.D. degree in nonlinear optics and its applications in deep learning from the National Research Council of Canada, University of Ottawa, Ottawa, ON, Canada, in 2021. From 2021 to 2024, he was a Research Scientist with few-cycle Inc., Varennes, QC, Canada. His research interests include the development of high-power ultrafast laser sources and algorithms for short pulse characterization.

Gabriel Tempea received the Graduation degree in technical physics from the Politechnica University, Bucharest, Romania, in 1996, and the Ph.D. degree from the Vienna University of Technology, Vienna, Austria, in 1999. He was a Research Assistant with the Vienna University of Technology till 2004. In 2002, he was a Postdoctoral Researcher with Université Bordeaux 1, Talence, France. From 2004 to 2018, he was a Product Manager with Femtolasers Produktions GmbH, Vienna. Since 2019, he has been a Senior Product Manager with few-cycle Inc., Varennes, QC, Canada. He has authored or coauthored 56 articles published in peer-reviewed scientific journals, two book-chapters, 54 reviewed conference-contributions, and four patents. His research interests include the generation and applications of femtosecond laser pulses.

François Légaré received the master's and Ph.D. degree in chemistry from the University of Sherbrooke, Sherbrooke, QC, Canada, in 2001 and 2004. From 2004 to 2006, he was a Postdoc with Harvard University, Cambridge, MA, USA. In 2006, he joined the Institut national de la recherche scientifique, Varennes, QC, Canada, as a Professor, where he has been a Full Professor since 2013. From 2013 to 2023, he has been the scientific head of the Advanced Laser Light Source (ALLS), Varennes. Since 2024, he has been the Director of INRS and a CEO of the ALLS facility. He has supervised 52 interns, 19 M.Sc. and 24 Ph.D. Students, and 24 Postdoctoral Fellows. He specializes in developing novel approaches for ultrafast science and technologies, and biomedical imaging with nonlinear optics.

Carlos A. Trallero-Herrero received the M.Sc. degree in nuclear physics from the Higher Institute for Nuclear Sciences and Technology, Havana, Cuba, in 2001, and the second M.Sc. degree in physics and the Ph.D. degree in physics from Stony Brook University, Stony Brook, NY, USA, in 2004 and 2007, respectively. During 2007–2010, he was a Postdoctoral Fellow with National Research Council Canada, Ottawa, ON, Canada, an Assistant Professor with Kansas State University, Manhattan, KS, USA, during 2010–2016, and an Associate Professor with Kansas State University, during 2016–2017. Since 2017, he has been an Associate Professor, and since 2022 a Full Professor at the Department of Physics, University of Connecticut, Storrs, CT. He is also an adjoint professor at the Department of Electrical and Computer Engineering at University of Connecticut, Storrs, CT. His research interests include attosecond science, strong field molecular spectroscopy, cohere control, higher-order harmonic generation, non-Gaussian optics, strong field science at long wavelengths, ultrafast optics.

Giulio Vampa received the B.Sc. degree in physics and the M.Sc. degree (*Summa cum Laude*) in solid state physics from Universita' degli Studi di Trieste, Trieste, Italy, in 2008 and 2010, respectively, and the Ph.D. degree in physics from the University of Ottawa, Ottawa, ON, Canada, in 2016. During 2016-2020, he was a Postdoctoral Fellow with Stanford PULSE Institute, Menlo Park, CA, USA. Since, 2020, he has been a Research Scientist with the National Research Council of Canada, Ottawa, ON, Canada and part of the Joint Attosecond Science Laboratory between NRC and the University of Ottawa, ON, Canada. He is also a Fellow of the Joint Center for Extreme Photonics and Adjunct Professor of physics with the University of Ottawa. His research interests include the fundamentals and the applications of attosecond science in materials, and nanostructured solids.

Bruno E. Schmidt received the Dipl.Ing. (FH) degree from the Cologne University of Applied Sciences, Colone, Germany, in 2003, and the Ph.D degree from Freie Universität Berlin, Berlin, Germany, in 2008. He was a Postdoctoral Researcher and then a Research Associate with INRS - Institut national de la recherche scientifique, Varennes, QC, Canada, during 2009–2013 and during 2013–2015, respectively. Since 2013, he has been the Founder and CTO of few-cycle Inc., Varennes, developing optical technologies for ultrafast laser science. His research interests include pulse post compression based on hollow-core fibers, frequency domain optical parametric amplification, fourier nonlinear optics, high-harmonic and terahertz generation, frequency-resolved optical gating.